Critical behavior of three interacting strings

Roland R. Netz and Reinhard Lipowsky

Institut für Festkörperforschung, Forschungszentrum Jülich, 5170 Jülich, Germany

(Received 8 October 1992)

The unbinding of three strings in a plane which interact via short-ranged attractive potentials is studied using both transfer-matrix methods and Monte Carlo techniques. In the symmetric case, for which the two outer strings have the same line tension, the critical behavior depends on the relative flexibility of the inner string in a nonuniversal fashion. In the asymmetric case, the strings unbind in two succcessive unbinding transitions at two different temperatures. Renormalization-group arguments predict that these results are also applicable to the adhesion and unbinding of three membranes.

The interactions of one-dimensional strings determine the behavior of domain walls in adsorbed monolayers, of steps or ledges on the surface of crystals, of vortex lines in type-II superconductors, and of bundles of rigid polymers such as double-helical or triple-helical biopolymers. Previous theoretical work on interacting strings has been primarily concerned with two cases: (i) The unbinding of two strings or domain walls which corresponds to wetting transitions. In this case, both *repulsive* and *attractive* interactions have been considered, which lead to various universality classes [1]. (ii) The unbinding of a large number of strings which interact, in this case, with purely *repulsive* interactions as in commensurate-incommensurate transitions. In the latter case, the strings are bound together by an external field or constraint.

On the other hand, there are several experimental systems in which one looks at the behavior of a bundle of more than two strings which also experience both repulsive *and* attractive interactions. For example, on vicinal surfaces, one often has attractive interactions between monoatomic steps which lead to multiple-atomic steps [2]. Likewise, some biopolymers such as collagen consist of three helices which form a bound state. In this case, the unbinding transition corresponds to the helix-coil transition [3].

Another system which has been studied recently consists of bunches of two-dimensional membranes which are bound together by van der Waals forces. In this case, unbinding transitions have been observed which were induced by a change in temperature [4]. In fact, bunches of membranes are expected to behave very similarly to bundles of strings. This is shown, using functional renormalization, at the end of this paper.

In the main part of this paper, we theoretically study the unbinding of three strings in two dimensions which interact by pairwise attractive and hard-wall repulsive forces. We find that this system exhibits a rich phase diagram, as shown schematically in Fig. 1. If the two outer strings of the bundle have different line tensions [5], two successive transitions are found: first, one string separates off from the other two, which then unbind at another transition at higher temperature. Both transitions exhibit

the same critical behavior which is universal and independent of the line tensions. In the phase diagram of Fig. 1, these two transitions occur at the two sheets which intersect at a line of tetracritical points. Along the latter line, the two outer strings of the bundle are identical. The critical behavior along this line is nonuniversal and depends on the ratio of line tensions of the inner and the outer strings.

The critical behavior of three interacting strings has been previously studied in an approximate way within the necklace model [6,7]. It is predicted that three identical strings undergo a *discontinuous* (or first-order) unbinding transition. In contrast, the work presented here clearly shows that the transition is in fact *continuous* (or second order) for a wide parameter range including the case of three identical strings.
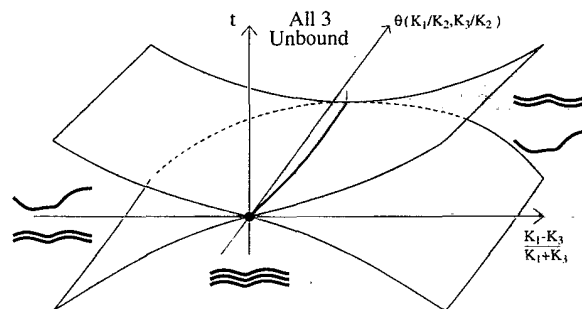

FIG. 1. The schematic phase diagram for the unbinding of three strings with arbitrary line tensions [in subregime (B)]. At the top (for high temperatures or low potential depths), all three strings are unbound; conversely, at the bottom, all three strings are tightly bound together. The four wings corresponding to universal unbinding transitions meet at a tetracritical line, on which the critical exponents vary continuously. For $\theta = \pi/2$, defining the plane containing the solid circle, the critical lines meet at a nonzero angle. As one moves back into the diagram (for decreasing θ), the scaling dimension of t increases, suggesting that the critical wings then meet *horizontally* with a common tangent.

The effective Hamiltonian for three strings is

$$\mathcal{H}\{l_1,l_2,l_3\} = \int dx \left\{ \frac{1}{2}K_1 \left[\frac{dl_1}{dx}\right]^2 + \frac{1}{2}K_2 \left[\frac{dl_2}{dx}\right]^2 \right.$$
$$+ \frac{1}{2}K_3 \left[\frac{dl_3}{dx}\right]^2 + V(l_1-l_2)$$
$$\left. + V(l_2-l_3) \right\} . \tag{1}$$

The strings are, on average, parallel to each other. The positive line tensions K_α can have different values. The

limit $K_\alpha = \infty$ corresponds to a hard wall. The two mutual interactions are chosen to be identical and given by

$$\frac{V(l)}{T} = \begin{cases} \infty & \text{for } l < 0 \\ -U & \text{for } 0 < l < l_0 \\ 0 & \text{for } l_0 < 1 , \end{cases} \tag{2}$$

with $U > 0$, corresponding to an attractive potential well.

The Hamiltonian can be simplified by an orthogonal transformation [7,8], which extracts the center of mass coordinate. The Hamiltonian (1) then becomes

$$\mathcal{H}\{y_1,y_2\} = \int dx \left\{ \frac{1}{2} \left[\left[\frac{dy_1}{dx}\right]^2 + \left[\frac{dy_2}{dx}\right]^2 \right] + V \left[\left[\frac{1}{K_1}+\frac{1}{K_2}\right]^{1/2} y_1 \right] + V \left[\left[\frac{1}{K_2}+\frac{1}{K_3}\right]^{1/2} (y_2\sin\theta - y_1\cos\theta) \right] \right\} , \tag{3}$$

where the center-of-mass coordinate, which diffuses freely, has been separated off. Using the ratios of the line tensions, denoted by $q_1=K_1/K_2$ and $q_3=K_3/K_2$, the angle θ is given by

$$\theta = \arctan(\sqrt{1/q_1+1/q_1q_3+1/q_3}) . \tag{4}$$

The problem of three strings in a two-dimensional plane with mutual square-well interactions has thus been transformed into the problem of one string in a three-dimensional wedge, with square-well potentials at the boundaries of the wedge.

For $q_1=q_3=0$, we get $\theta=\pi/2$, and the Hamiltonian decouples into two independent problems, which can be solved exactly [1]. For three identical strings with $q_1=q_3=1$, we get $\theta=\pi/3$; as the inner string becomes more flexible, q_1 and q_3 increase and the angle θ of the wedge decreases.

We have carried out Monte Carlo (MC) simulations of this Hamiltonian for a system consisting of 500 discrete sites using the Metropolis algorithm with periodic boundary conditions. Runs were typically of the order of 10^7 MC steps per site. The mean string separations, $\langle l_{12}\rangle \equiv \langle l_1-l_2\rangle$ and $\langle l_{23}\rangle \equiv \langle l_2-l_3\rangle$, were measured, where $\langle \ \rangle$ represents an ensemble average. For the symmetric case, we have $\langle l_{12}\rangle=\langle l_{23}\rangle$; we then used $\langle l\rangle \equiv (\langle l_{12}\rangle+\langle l_{23}\rangle)/2$, and the roughness $\xi_\perp$ was determined by evaluating $\xi_\perp=[(\langle l_{12}^2\rangle-\langle l_{12}\rangle^2)^{1/2} +(\langle l_{23}^2\rangle-\langle l_{23}\rangle^2)^{1/2}]/2$. We also determined the parallel correlation length $\xi_\parallel$ [9].

For the transfer-matrix (TM) calculation, which amounts to a numerical iteration of the Schrödinger equation corresponding to the Hamiltonian (3), we also discretize the coordinates y_1 and y_2, using 80 000 sites. This discretization deserves special attention and has to be done in accord with several symmetry conditions [9]. Using the restricted solid-on-solid approximation (RSOS), the Schrödinger equation was iterated 20 000 times using a fully vectorized code, after which we obtained a stationary probability distribution. From this

distribution, we calculated the mean string separations and the roughness. The energy E_0 of the ground state can be obtained (up to a constant) via the numerically determined eigenvalue of the TM. The parallel correlation length is then given by $\xi_\parallel=T/(E_1-E_0)$, where E_1 is the energy of the first excited state. The restriction to nearest neighbors should not change the critical behavior. This is well established for the case $\theta=\pi/2$. We also confirmed this for the Schrödinger equation corresponding to the necklace model for the angles $\theta=\pi,\pi/2$, $2\arctan(\frac{1}{2})$, and $2\arctan(\frac{1}{3})$ by comparing the numerically determined critical exponents with those obtained analytically [9].

To study the unbinding transition, we fixed the values of K_α/T and the potential well width $l_0=1$, and varied the depth of the potential well U, decreasing it toward the critical value U_c. The presence of the inner string should result in an entropically generated effective potential V_R between the two outer strings which is repulsive and scales as $V_R \sim 1/l^2$. Intuitively, it is clear that as one increases the ratio of the line tensions of the outer and inner strings, the thermal fluctuations of the central string increase, leading to an increased amplitude W of the repulsive effective potential. Theoretical results for the unbinding of two strings in the presence of a repulsive potential $V_R=W/l^2$ imply that the lengths defined above scale as

$$\langle l\rangle \sim (U-U_c)^{-\psi} ,$$
$$\xi_\perp \sim (U-U_c)^{-\nu_\perp} , \tag{5}$$
$$\xi_\parallel \sim (U-U_c)^{-\nu_\parallel} ,$$

where the exponents are found to depend on the rescaled amplitude $w=2KW/T^2$ in the following way [1]: for subregime (B), with $0<w<\frac{1}{4}$, the exponents satisfy the simple relation $\psi=\nu_\perp=\nu_\parallel/2$ and

$$\psi=(1+4w)^{-1/2} ; \tag{6}$$

in subregime (C), with $w > \frac{3}{4}$, one has $\nu_{\parallel} = 1$ and $\psi < \nu_{\perp} < \frac{1}{2}$ or discontinuities in $\langle l \rangle$ and $\xi_{\perp}$.

First, we report on our results for the *symmetric* case, i.e., $q_1 = q_3 \equiv q$, where the strings unbind simultaneously. The first set of TM calculations has been carried out for $\theta = \pi/2$ or $q = 0$, which corresponds to the central string being a hard wall. Since this string does not fluctuate, the amplitude of the effective repulsive potential has to be zero and $\psi = \nu_{\perp} = 1$, according to (6). The data for the three lengths were fitted to a power law using the Levenberg-Marquardt method for a three-parameter fit [9]. The data, which are shown in a log-log plot in Fig. 2(a), scale accurately with $\psi = 1.01 \pm 0.01$ and $\nu_{\perp} = 0.99 \pm 0.01$, thus confirming the theoretical prediction with high precision. For fitting the parallel correlation length $\xi_{\parallel}$, we also had to determine the energy E_1 of the first excited state; the data are therefore not as reliable and yield $\nu_{\parallel} = 1.8 \pm 0.2$, which is to be compared with the theoretical prediction $\nu_{\parallel} = 2$.

In addition, we performed eight TM calculations for different nonzero values of q. In Fig. 2(b), we show the data for $q = 31.5$, which corresponds to an angle of $\theta = 2 \arctan(\frac{1}{8})$. The same high accuracy is obtained, yielding the exponents $\psi = 0.707 \pm 0.005$ and $\nu_{\perp} = 0.712 \pm 0.005$. Thus the effective repulsive potential induced by the fluctuations of the inner string actually changes the critical behavior. Following (6), one calcu-
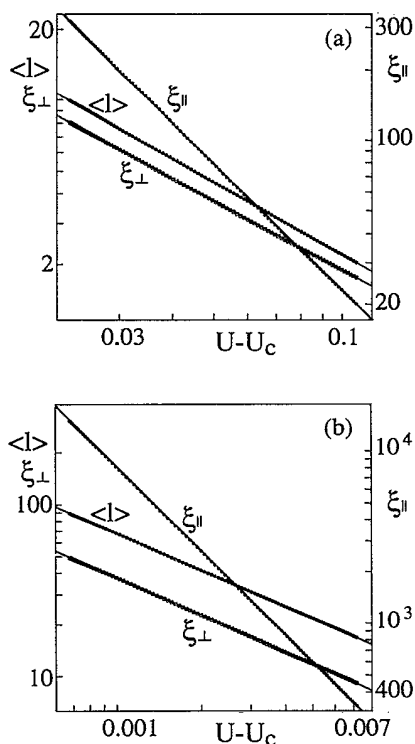

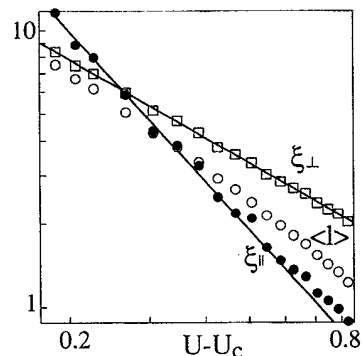FIG. 3. Monte Carlo results for $q = 1.0$ and $K_2 = 0.1$. Shown are data for the roughness (open squares), the parallel correlation length (closed circles), and the mean separation $\langle l \rangle$ (open circles).

lates the amplitude of this potential to be $w(q = 31.5) \simeq 0.25$; the critical behavior still belongs to the subregime (B), as confirmed by the fact that the two exponents are the same within their numerical errors.

MC simulations have been carried out for $q = 1$ $(\theta = \pi/3)$, where all strings have the same line tension $K_\alpha/T = 0.1$. The data, which are shown in Fig. 3, yield $\nu_{\perp} = 0.93 \pm 0.05$ and $\nu_{\parallel} = 1.8 \pm 0.2$, thus confirming scaling predictions. The mean separation $\langle l \rangle$ does not scale as nicely, but approaches the slope of the roughness $\xi_{\perp}$ close to the transition. It turns out that the MC simulation of a single data point in Fig. 3 requires twice as much computer time as the calculation of about 100 data points in Fig. 2(a), using the TM technique.

The measured values of ψ and $\nu_{\perp}$ are plotted as a function of θ in Fig. 4. Apart from some deviations which are probably due to the presence of crossover effects, the two exponents show the same behavior. The MC result agrees with the TM results within the error bar. For $\theta = \pi/2$, the exact result (indicated by a cross) is reproduced. For decreasing angle, the exponents decrease. For the smallest angle considered here, $\theta = 2 \arctan(\frac{1}{12})$,

FIG. 2. (a) Transfer-matrix results for $K_2 = \infty$ and $K_1 = K_3$ ($q = 0$ and $\theta = \pi/2$). Data for the parallel correlation length $\xi_{\parallel}$, the mean separation $\langle l \rangle$, and the roughness $\xi_{\perp}$ are shown as a function of the potential depth U. (b) Results for $K_1/K_2 = K_3/K_2 = 31.5$.
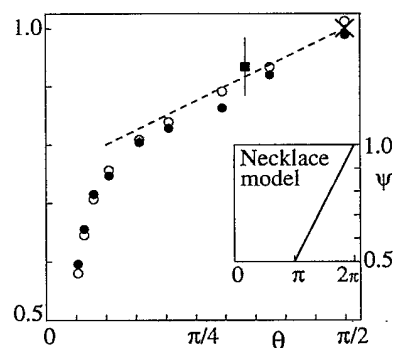

FIG. 4. Results for the exponents ψ (open symbols) and $\nu_{\perp}$ (filled symbols). The square denotes the Monte Carlo result for $\nu_{\perp}$, the circles denote transfer-matrix results. In the latter case, the error bars are the size of the symbols. The cross denotes the exactly known result for the case $\theta = \pi/2$, namely $\psi = \nu_{\perp} = 1$. The inset shows the results for the necklace model, with discontinuous transitions for $\theta < \pi$.

which corresponds to $q=71.5$, the border to subregime (C), at which $\psi=0.5$, has not been reached. In fact, by plotting the amplitude of the effective repulsive potential, w, as calculated via (6), as a function of q, we estimate from linear extrapolation that the transition to subregime (C) occurs only for $q \simeq 130$. This gentle change of the critical behavior helps to understand very recent MC simulations [8], where the unbinding of three membranes was found to exhibit critical exponents only slightly different from those for two membranes.

The exponent ψ in the inset of Fig. 4 has been obtained using a rigorous solution of the Schrödinger equation corresponding to the necklace model [7,9]. Within the latter model, the borderline between subregimes (B) and (C) is at $\theta=\pi$, and the unbinding of three strings, for which $0 < \theta < \pi/2$ is predicted to proceed always via a strongly discontinuous transition. This does not agree with the exact solution for $\theta=\pi/2$, which gives a continuous transition with $\psi=1$. The broken line in Fig. 4 gives the results of an improved necklace model, where we adjusted the boundary conditions for the Schrödinger equation in such a way that the exact result for $\theta=\pi/2$ is recovered [9]. This curve agrees well with our numerical data in the vicinity of $\theta=\pi/2$.

The critical temperature decreases as an inverse square root with the tension ratio q for fixed K_1 and K_3. By linear interpolation, we estimate $T_c(q=0)/T_c(q=1) \simeq 1.5$.

In Fig. 1, the point denoted by a filled circle corresponds to the critical symmetric case, with $\theta=\pi/2$ and $\psi=1$. As one softens the inner string (and the angle θ decreases), one moves back into the diagram. The vertical axis measures temperature (or inverse potential strength) in reduced units of $t \equiv [T/l_0^2 U(K_1+K_3)]^{1/2}$; note that a factor of $1/T$ has been adsorbed in the definition of U.

Now consider the *asymmetric* case with $K_1 \neq K_3$. For $K_2=\infty$, one has $\theta=\pi/2$ and the corresponding Schrödinger equation can again be solved exactly: In this case, the two outer strings unbind from the wall at two different temperatures, the ratio of which is given by $T_c^{(12)}/T_c^{(23)}=\sqrt{K_1/K_3}$. In order to check the corresponding behavior for finite K_2, we performed three TM

calculations for $q_3=\infty$ and $q_1=1, 4$, and 9, respectively. This corresponds to a stack of two strings on top of a rigid wall. Here we find two distinct unbinding transitions. We conclude that the unbinding proceeds via two separate transitions for all values of θ as soon as $K_1/K_3 \neq 1$. The transitions are then characterized by the universal exponent $\psi=1$. In Fig. 1, the four wings of these universal transitions come together at the locus denoted by the bold line, which is a line of tetracritical points. Apart from the decoupled case with $q=0$, this line should lead to a nontrivial crossover from universal to nonuniversal critical behavior.

Finally, the effective Hamiltonian as given by (3) can also be studied by functional renormalization-group methods [10]. For infinitesimal rescaling factor $b \approx 1 + \Delta t$, one obtains [9]

$$\frac{1}{\zeta}\frac{\partial U}{\partial t} = \tau U + y_\alpha \partial_\alpha U + \ln \det(\delta_{\alpha\beta} + \partial_\alpha \partial_\beta U) , \qquad (7)$$

where the two-dimensional potential $U(\mathbf{y})$ is a rescaled superposition of the mutual interactions in (3). For strings in two dimensions, one has $\zeta=\frac{1}{2}$ and $\tau=2$. The flow equation (7) also applies to fluid membranes in three dimensions with $\zeta=1$ and $\tau=2$. Since $\tau=2$ in both cases, the fixed points, defined by $\partial U/\partial t=0$, are identical, and the critical exponents are related in a trivial way. Thus our results obtained for three strings should also be applicable to three interacting membranes, as confirmed by recent MC simulations of three fluid membranes [8,9].

Very recently, two mean-field-type calculations for the simultaneous unbinding of a stack of membranes have been described [11,12], which predict *universal* critical behavior, in contrast to the results presented here.

Note added: The problem of n identical strings $(n > 2)$ has also been studied via an approximate mapping onto a quantum spin chain [13], which also leads to n-independent critical behavior.

[1] R. Lipowsky, Physica A **177**, 182 (1991); R. Lipowsky and T. M. Nieuwenhuizen, J. Phys. A **21**, L89 (1988).

[2] C. M. Schneider, P. Bressler, J. Kirschner, J. J. de Miguel, and R. Miranda, Phys. Rev. Lett. **64**, 1059 (1990); J. Frohn, M. Giesen, M. Poensgen, J. F. Wolf, and H. Ibach, *ibid.* **67**, 3543 (1991).

[3] D. Poland and H. A. Scheraga, J. Chem. Phys. **45**, 1464 (1966).

[4] W. Helfrich and M. Mutz, in *Random Fluctuations and Growth*, edited by H. E. Stanley and N. Ostrowsky (Kluwer, Dordrecht, 1988); M. Mutz and W. Helfrich, Phys. Rev. Lett. **62**, 2881 (1989).

[5] Here and below, we use the term "line tension" even if the system is anisotropic and the term "line stiffness" would

be more appropriate.

[6] M. E. Fisher, J. Stat. Phys. **34**, 667 (1984); D. A. Huse and M. E. Fisher, Phys.Rev. B **29**, 239 (1984).

[7] M. E. Fisher and M. Gelfand, J. Stat. Phys. **53**, 175 (1988).

[8] J. Cook-Röder and R. Lipowsky, Europhys. Lett. **18**, 433 (1992).

[9] The details of our methods will be presented in R. R. Netz and R. Lipowsky (unpublished).

[10] R. Lipowsky and M. E. Fisher, Phys. Rev. B **36**, 2126 (1987); R. Lipowsky, Phys. Rev. Lett. **62**, 704 (1989).

[11] S. T. Milner and D. Roux, J. Phys. I France **2**, 1741 (1992).

[12] W. Helfrich, J. Phys. II France **3**, 385 (1993).

[13] T. W. Burkhardt and P. Schlottmann (unpublished).